Cerebral Cortex Communications, 2020, **1**, 1–16

doi: 10.1093/texcom/tgaa052
Original Article

ORIGINAL ARTICLE

In-Depth Characterization of Layer 5 Output Neurons of the Primary Somatosensory Cortex Innervating the Mouse Dorsal Spinal Cord

N. Frezel[1], E. Platonova[2], F. F. Voigt[3,4], J. M. Mateos[2], R. Kastli[3,4], U. Ziegler[2], T. Karayannis[3,4], F. Helmchen[3,4], H. Wildner[1] and H. U. Zeilhofer[1,5]

[1]Institute of Pharmacology and Toxicology, University of Zurich, CH-8057 Zürich, Switzerland, [2]Center for Microscopy and Image Analysis, University of Zurich, CH-8057 Zürich CH-8057, Switzerland, [3]Brain Research Institute, University of Zurich, CHJ-8057 Zurich CH-8057 , Switzerland, [4]Neuroscience Center Zurich, University of Zurich and ETH Zurich, CH-8057 Zurich CH-8057, Switzerland and [5]Institute of Pharmaceutical Sciences, Swiss Federal Institute of Technology (ETH Zürich), CH-8090 Zürich, Switzerland

Address correspondence to Dr. H. U. Zeilhofer, Institute of Pharmacology and Toxicology, University of Zurich, Winterthurerstrasse 190, CH-8057 Zürich, Switzerland. Email: zeilhofer@pharma.uzh.ch and Dr. H. Wildner. Email: hwildner@pharma.uzh.ch.

Abstract

Neuronal circuits of the spinal dorsal horn integrate sensory information from the periphery with inhibitory and facilitating input from higher central nervous system areas. Most previous work focused on projections descending from the hindbrain. Less is known about inputs descending from the cerebral cortex. Here, we identified cholecystokinin (CCK) positive layer 5 pyramidal neurons of the primary somatosensory cortex (CCK $^+$ S1-corticospinal tract [CST] neurons) as a major source of input to the spinal dorsal horn. We combined intersectional genetics and virus-mediated gene transfer to characterize CCK$^+$ S1-CST neurons and to define their presynaptic input and postsynaptic target neurons. We found that S1-CST neurons constitute a heterogeneous population that can be subdivided into distinct molecular subgroups. Rabies-based retrograde tracing revealed monosynaptic input from layer 2/3 pyramidal neurons, from parvalbumin positive cortical interneurons, and from thalamic relay neurons in the ventral posterolateral nucleus. Wheat germ agglutinin-based anterograde tracing identified postsynaptic target neurons in dorsal horn laminae III and IV. About 60% of these neurons were inhibitory and about 60% of all spinal target neurons expressed the transcription factor c-Maf. The heterogeneous nature of both S1-CST neurons and their spinal targets suggest complex roles in the fine-tuning of sensory processing.

Key words: AAV-based viral tracing, CCK, corticospinal tract, dorsal spinal cord, somatosensory cortex

Introduction

In addition to the hindbrain, the cerebral cortex is a major source of descending input to the spinal cord (Lemon and Griffiths 2005; Abraira et al. 2017; Wang et al. 2017; Liu et al. 2018; Ueno et al. 2018). Layer 5 pyramidal neurons of several cortical areas project to this site, including neurons residing in the motor and premotor cortices as well as in the somatosensory cortex (S1). In rodents

Received: 7 July 2020; **Revised:** 7 July 2020; **Accepted:** 9 August 2020

as well as in humans, the axons of the corticospinal tract (CST) neurons travel through the internal capsule in the forebrain to enter the cerebral peduncles at the base of the midbrain. They then pass through the brainstem to form the pyramids, at the base of the medulla. The vast majority of the fibers decussate at this level to enter the spinal cord. From there, the axons of the rodent CST run in the ventral part of the dorsal funiculus, while in humans the tract is located in the lateral white matter.

Most studies on the function of the CST have focused on fine motor control (Wang et al. 2017; Ueno et al. 2018) often in the context of spinal cord injury and spinal cord repair (Bareyre et al. 2005; Steward et al. 2008; Fry et al. 2010; Porrero et al. 2010; Jin et al. 2015). These studies have targeted either the whole CST, or CST neurons of the motor cortex. The presence of direct synaptic contacts between CST neurons that descend from S1 and spinal interneurons (Abraira et al. 2017; Liu et al. 2018; Ueno et al. 2018) suggests that CST neurons also play an important role in somatosensory processing, beyond sensorimotor integration. This is in line with previous findings that CST neurons from the motor (M1) and S1 cortices contact distinct populations of spinal interneurons (Ueno et al. 2018).

The functional analysis of specific parts of the CST has been in part limited by the lack of tools to specifically target defined subgroups of CST neurons (e.g., CST neurons that descend from a defined cortex area to a specific spinal cord region). Transgenic mouse lines (Bareyre et al. 2005; Porrero et al. 2010) and virus-mediated gene transfer (Hutson et al. 2012; Ueno et al. 2018) have been used to label axons and terminals of CST neurons in the spinal cord. These studies and earlier tracing studies (Casale et al. 1988) showed that the CST axons terminate mainly in the laminae III and IV of the dorsal horn, where they contact dorsal horn interneurons (Abraira et al. 2017; Ueno et al. 2018). However, the Emx1 or Thy1-H fluorescent reporter mice used in these studies label many neurons in addition to CST neurons (Bareyre et al. 2005; Porrero et al. 2010; Willenberg and Steward 2015; Zeisel et al. 2015), and therefore do not allow specific targeting of CST neurons for characterization and functional manipulation. To this end, it will be crucial to restrict transgene expression to the layer 5 pyramidal neurons in an area of the cortex (S1 in this case) that projects to the spinal region of interest such as the dorsal horn. Recently, a new recombinant adeno-associated virus (rAAV) serotype (rAAV2-retro) (Tervo et al. 2016) has been developed with greatly improved retrograde labeling efficacy that allows high fidelity tracing of descending inputs to the spinal cord (Haenraets et al. 2017; Wang et al. 2018).

Here, we developed a combination of viral approaches and transgenic mice to specifically label S1-CST neurons. This approach permitted the expression of fluorescent or effector proteins in S1 cortical neurons that project directly to a predefined region of the spinal cord and allowed us to demonstrate that S1-CST neurons with terminations in the spinal dorsal horn constitute a heterogeneous population of neurons that receive monosynaptic input from forebrain sensory circuits and target dorsal horn interneurons known to be involved in the gating of somatosensory and nociceptive signals.

Methods

Animals

Experiments were performed on 6–12-week-old mice kept at a 12:12 h light/dark cycle. Permissions for experiments have been obtained from the Canton of Zurich (permissions 03/2018, 031/2016, and 063/2016). CCK^{Cre} mice (Cck<tm1.1(cre)Zjh>/J, Taniguchi et al. 2011) were purchased from Jackson Laboratory. For further details on the genetically modified mice used in this study, see Table 1.

Immunohistochemistry

Mice were transcardially perfused with 4% ice-cold paraformaldehyde (PFA, in 0.1 M sodium phosphate buffer, pH 7.4). Lumbar spinal cord and brain were immediately dissected and postfixed for 2.5 h with 4% PFA on ice. Postfixed tissue was briefly washed with 0.1 M sodium phosphate buffer (pH 7.4) and then incubated in 30% sucrose (in phosphate buffered saline – PBS) overnight at 4°C for cryoprotection. Cryoprotected tissue was cut at 25 µm or 40 µm (spinal cord or brain, respectively) on a Hyrax C60 Cryostat (Zeiss), mounted on superfrost plus glass slides and then incubated with the respective combinations of primary antibodies in 1% donkey serum in PBS over-night at 4°C. After brief washes in PBS, sections were incubated with the respective secondary antibodies for 2 h at room temperature and briefly rinsed in PBS, before mounting with coverslips and DAKO fluorescent mounting media (Dako). Secondary antibodies raised in donkey were purchased from Jackson Immuno Research. All primary antibodies used are listed in Table 1.

Multiplex In Situ Hybridization and Image Analysis

Spinal tissue used for in situ hybridization (ISH) was dissected from 6 to 12-week-old mice, collected in 1.5 mL Eppendorf tubes, and immediately frozen in liquid nitrogen. Tissue was embedded in NEG50 frozen section medium (Richard-Allen Scientific), cut into 16 µm thick sections, and hybridized using the probes designed for RNAscope Fluorescent Multiplex ISH listed in Table 1.

For immunohistochemistry and ISH, Z-stacks of fluorescent images were acquired on a Zeiss LSM700 confocal and a Zeiss LSM800 Airy Scan microscope (Zeiss). Numbers of immunoreactive cells in z-stacks were determined using the ImageJ (NIH) Cell Counter plugin (Kurt DeVos, University of Sheffield, Academic Neurology).

Intraspinal and Cortical Virus Injections

Viruses were obtained from the resources indicated in Table 1 and used as previously described (Haenraets et al. 2017). Virus injections were made in adult (6–8-week-old) mice anesthetized with 2% isoflurane and immobilized on a motorized stereotaxic frame (David Kopf Instruments and Neurostar). For intraspinal injections, the vertebral column was fixed using a pair of spinal adaptors and lumbar spinal cord at L4 and L5 was exposed. Injections (3 × 300 nL) spaced approximately 1 mm apart were made at a rate of 50 nL/min with glass micropipettes (tip diameter 30–40 µm) attached to a 10 µL Hamilton syringe. For S1 injections, the head was fixed using head bars, the skull exposed and the following injection coordinates were used: (Bregma −1 mm; midline +1.5 mm; depth: 0.8 mm).

Tissue Clearing and Light Sheet Imaging

In order to label the CST neurons more sparsely, we injected an AAV-DJ/2.Dre into the lumbar spinal cord instead of the rAAV2-retro in order to get sparse labeling of CST neurons and better visualization of individual neurons and axons in cleared brains. Three weeks after viral injections, mice were deeply anesthetized using pentobarbital and perfused transcardially with

Table 1. Materials and reagents

Materials	Resource	Identifier
Mice (shortname)		
C57BL/6J (wild type)	The Jackson Laboratory	IMSR_JAX:000664
C57BL/6.FVB-Tg(Slc6a5-EGFP)13Uze (GlyT2::eGFP)	IPT (Zurich, Switzerland)	MGI:3835459, Zeilhofer et al. (2005)
Cck<tm1.1(cre)Zjh>/J (CCK^{Cre})	Jackson Laboratory	Taniguchi et al. (2011)
Viral vectors short name		
rAAV-retro/2-shortCAG-dlox-EGFP	VVF (Zurich, Switzerland)	This publication (vHW22-retro)
rAAV-retro/2-shortCAG-tdTomato	VVF (Zurich, Switzerland)	v131-retro
rAAV-retro/2-hEF1a-DreO	VVF (Zurich, Switzerland)	v127-retro
ssAAV-DJ/2-hEF1a-DreO	VVF (Zurich, Switzerland)	v127-DJ
rAAV-9/2-hEF1α-D_{on}/C_{on}-EGFP	VVF (Zurich, Switzerland)	This publication (vHW18–1)
rAAV-retro/2-hCMV-Cre	VVF (Zurich, Switzerland)	v36-retro
rAAV1-CAG-flex.eGFP	Penn Vector Core (Philadelphia, USA)	V3675TI-Pool
rAAV-8/2-hSyn1-roxSTOP-dlox-TVA_2A.RabG	VVF (Zurich, Switzerland)	This publication (vHW7–1)
SAD.RabiesΔG.eGFP (EnvA) (EnvA.RV.dG.eGFP)	Salk Institute (La Jolla, CA, USA)	Albisetti et al. (2017)
AAV1-CAG-flex-tdTom	Penn Vector Core (Philadelphia, USA)	AllenInstitute854
rAAV2-EF1α-flex-WGA	IPT (Zurich, Switzerland)	This publication
ssAAV-1/2-hSyn1-dlox-mSyp1-EGFP	VVF	vHW41.1
Primary antibodies (dilution)		
Goat anti-Pax2 (1:400)	R&D Systems (Minneapolis, MN, USA)	AB_10889828
Guinea pig anti-Lmx1b (1:10 000)	Dr Carmen Birchmeier	Muller et al. (2002)
Chicken anti-GFP (1:1000)	Life Technologies (Carlsbad, CA, USA)	AB_2534023
Rabbit anti-GFP (1:1000)	Molecular Probes (Eugene, OR, USA)	AB_221570
Rabbit anti-NeuN (1:1000)	Abcam (Cambridge, UK)	AB_10711153
Guinea pig anti-NeuN (1:1000)	Synaptic System (Göttingen, D)	AB_2619988
Goat anti-WGA (1:2000)	VECTOR laboratories (Burlingame, CA, USA)	AS-2024
Rabbit anti-WGA (1:2000)	Sigma Aldrich (Saint-Louis, MO, USA)	T4144
Rabbit anti-c-Maf (1:1000)	Dr Carmen Birchmeier	#40
Guinea pig anti-c-Maf (1:1000)	Dr Carmen Birchmeier	#2223, #1 Final bleed
Rabbit anti-PKCg (1:1000)	Santa Cruz (Dallas, Texas, USA)	AB_632234
Rabbit anti-SST (1:1000)	Santa Cruz (Dallas, Texas, USA)	sc-13099
Mouse anti-PV (1:1000)	Swant (Marly, Switzerland)	235
Guinea pig anti-PV (1:1000)	Immunostar (Hudson, WI)	24428
Rabbit anti-NPY (1:1000)	Peninsula Laboratories (San Carlos, CA, USA)	T-4069
Rabbit anti-TVA	Dr Sauer	Seidler et al. (2008)
Goat anti-tdTomato (1:1000)	Sicgen (Cantanhede, Portugal)	AB8181-200
Rabbit antihomer	Synaptic System (Göttingen, D)	AB_2120990
Guinea pig antihomer	Synaptic System (Göttingen, D)	AB_10549720
RNAscope multiplex FISH probes		
CCK	ACD	Mm-CCK-C1
CRE	ACD	CRE-C3
GFP	ACD	Mm-GFP-C3
RORα	ACD	Mm-Rora-C2
Crhr1	ACD	Mm-Crhr1-C2
Etv1 (Er81)	ACD	Mm-Etv1-O1-C1
Bcl11b (Ctip2)	ACD	Mm-Bcl11b-C1
Htr2c (5-HTR2c)	ACD	Mm-Htr2c-C1
$GABAR_{\gamma}1$	ACD	Mm-Gabrg1-C1
Plxnd1	ACD	Mm-Plxnd1
Nr4a2 (Nurr1)	ACD	Mm-Nr4a2-C1
Triplex positive control probe	ACD	3-plex Positive Control Probe- Mm
Triplex negative control probe	ACD	3-plex Negative Control Probe- Mm

Notes: IPT: Institute of Pharmacology and Toxicology, University of Zurich; VVF: Viral Vector Facility (University of Zurich; www.vvf.uzh.ch)

10 mL of ice cold PBS followed by 20 mL of ice-cold hydrogel solution (40% acrylamide, 2% bis-acrylamide, 10% VA-044 initiator, PBS, 16% PFA and dH_2O (Chung et al. 2013). Whole central nervous system (CNS; brains and with spinal cords attached) were dissected on ice and incubated in hydrogel solution for 24 h. Oxygen was removed using a desiccator and N_2 used to replace it to allow a good polymerization. Sampled were incubated for 3 h at 39.5°C for acrylamide polymerization, and then incubated in Sodium dodecyl sulfate (8% SDS, 200 mM boric acid and sodium hydroxide to adjust the pH at 8.5, Chung et al. 2013), at room temperature (RT) for passive clearing. After 8–9 weeks, the samples were washed in PBS at least 3 times for 4 h and then incubated in Histodenz-Triethanolamine solution (~80% Histodenz D2158 (Sigma-Aldrich), 11.5 mM PB, 5.7% Na-azide, 5.7% Tween 20 and ~30% Triethanolamine, pH 7.5; refractive index adjusted to 1.457) for 7 days. Finally, samples were

mounted in quartz cuvettes ($10 \times 20 \times 45$ mm^3, Portmann Instruments) for imaging in the same solution. Images were acquired using a mesoSPIM light-sheet microscope ("mesoscale selective plane illumination microscope," see mesospim.org) (Voigt et al. 2019). Briefly, samples were illuminated with an axially scanned light-sheet using an Omicron SOLE-6 laser engine at 488- and 561-nm excitation wavelengths. 3D stacks were generated by translating the sample through the light sheet. In the detection path, fluorescence signals were acquired with an Olympus MVX-10 microscope with a MVPLAPO 1x objective and a Hamamatsu Orca Flash 4.0 CMOS camera. Image analysis was performed with Fiji and Imaris (version 9.5.1, Bitplane AG).

Quantification of Retrogradely Labeled Neurons

For the quantification of the retrogradely labeled neurons using rabies virus, percentage of parvalbumin (PV) and somatostatin (SST) neurons were counted as percentage of GFP+(green fluorescent protein) TVA- (Tva receptor) neurons. Because of the lack of suitable antibodies, it was not possible to costain for neuropeptide Y (NPY) and TVA in the same section. Therefore percentage is expressed as percentage of all GFP$^+$ neurons. However, since we only found a single NPY and GFP positive neuron in the brains of 3 mice (196 neurons), we are confident that the main conclusions are not affected. Finally, pyramidal layer 2/3 neurons were identified based on their localization and morphology.

Experimental Design and Statistical Analysis

Cells counts are reported as mean ± standard error mean (SEM). Numbers of experiments (mice and cells) are provided in the figure legends.

Results

Labeling S1-CST Neurons in CCK^{Cre} Mice

CST neurons are the subset of excitatory long-range pyramidal projection neurons in layer 5 of the somatosensory cortex that terminate in the dorsal spinal horn where they release glutamate as their fast neurotransmitter. However, whether S1-CST neurons constitute a molecularly or functionally homogeneous population is unclear. Recent work (Zeisel et al. 2015) indicates that the neuropeptide cholecystokinin (CCK) is also expressed in some layer 5 neurons of S1. We therefore addressed the question whether and, if so, to what extend CST neurons in S1 express CCK. To specifically label CCK expressing CST neurons in S1, we injected transgenic mice carrying a knock-in Cre coding sequence in the CCK locus (CCK^{Cre} mice, Taniguchi et al. 2011) with a rAAV optimized for transduction through axons and axon terminals (rAAV2-retro) (Tervo et al. 2016). We have previously shown that spinal injection of rAAV2-retro vectors into the lumbar spinal dorsal horn transduces CST neurons in the primary sensory cortex (S1) via infection of their spinal axon terminals (Haenraets et al. 2017). We therefore repeated our initial experiments in CCK^{Cre} mice. First, we confirmed that Cre expression in these mice is restricted to CCK expressing cells (98.8 ± 0.4% of Cre$^+$ cells expressed CCK and 98.6 ± 0.7% of CCK$^+$ cells expressed Cre, Supplementary Fig. 1) using multiplex ISH. We then injected a rAAV2-retro encoding a Cre-dependent enhanced green fluorescent protein (AAV2-retro.flex.eGFP) into the spinal cord of these mice (Fig. 1A). This strategy uncovered a population of layer 5 pyramidal neurons in the primary somatosensory cortex that projects directly to the spinal dorsal horn (Fig. 1B and Supplementary Fig. 2A,B). We also found labeled neurons in a few other brain areas, including the anterior cingulate cortex, the thalamus, and the rostral ventromedial medulla (RVM) (Fig. 1B and Supplementary Fig. 2C–G). However, in all subsequent experiments, we focused on our initial central aim, the characterization of CST neurons in the somatosensory cortex. We tested whether all CST neurons in S1 expressed CCK^{Cre} or whether the CCK^{Cre} neurons were a subset of CST neurons. To this end, we coinjected a Cre dependent (rAAV2-retro.flex.eGFP) and a Cre independent rAAV2-retro (rAAV2-retro.tdTomato) into the lumbar spinal cord of CCK^{Cre} mice (Fig. 1C). eGFP would then be expressed in CCK^{Cre} positive S1-CST neurons, whereas tdTom would label all virus infected neurons projecting to the injection site. We found that about 70% (71.5 ± 3.1%) of the tdTom$^+$ S1-CST neurons also expressed eGFP. The proportion eGFP$^+$ neurons that expressed tdTomato was very similar (75.5 ± 1.6%, Fig. 1D). These values are consistent with an expression of CCK^{Cre} in the great majority of S1-CST neurons that project to the injection site. S1-CST neurons can hence be efficiently labeled using rAAV2-retro injections into the dorsal horn of CCK^{Cre} mice. CCK is not only expressed in cortical layer 5 pyramidal neurons of the mouse cortex but also in large subsets of excitatory and inhibitory neurons of the cerebral cortex (Xu et al. 2010; Zeisel et al. 2015). This also became apparent when we injected rAAVs containing a Cre-dependent tdTomato expression cassette directly into the S1 cortex (Fig. 1E,F). As a consequence, injection of rAAVs carrying Cre dependent reporter cassettes into CCK^{Cre} mice allows anterograde labeling of S1-CST terminals from the cortex and retrograde labeling of their somata from the spinal cord (Fig. 2A). It does however not permit a specific transduction of CST neurons from either of the 2 injection sites alone.

Viral Targeting Strategies to Label S1-CST Neurons

To overcome this limitation, we developed an intersectional strategy (Fig. 2) to specifically target CCK$^+$ neurons that project from S1 to the spinal cord. To this end, we injected a rAAV2-retro encoding for the Dre recombinase into the lumbar spinal cord of CCK^{Cre} mice (Fig. 2B). Subsequently, transduced S1-CST neurons (as well as other CCK^{Cre} neurons with processes or somata in the spinal cord) will express both recombinases. Using this strategy, we achieved targeted expression of the desired transgene by local injection of rAAVs carrying Cre- and Dre-dependent transgenes into S1. As a proof of principle, we demonstrate that this strategy works with the injection of a Cre- and Dre-dependent rAAV carrying the eGFP transgene (AAV.hEF1α.C$_{on}$/D$_{on}$.eGFP) into S1 (Fig. 2B and Supplementary Fig. 3). We did not detect eGFP expression outside of S1.

A possible variation of this intersectional strategy is the injection of a rAAV2-retro.Cre into the spinal cord of wild-type mice, followed by the local injection of a rAAV carrying a Cre-dependent transgene into S1 (Fig. 2C). As CCK^{Cre} positive neurons represent the vast majority of the S1-CST population, the 2 strategies should label the same neuron population in this particular case. Quantification of the different injection strategies shows that a single injection of rAAV2-retro.tdTom into the spinal cord of wild type mice (Fig. 2A,D) led to labeling of a similar number of neurons as compared with the C$_{on}$/D$_{on}$ strategy in CCK^{Cre} mice (Fig. 2B,D). Targeting S1-CST neurons by spinal injection of rAAV2-retro.Cre in wild-type mice, followed by the local injection of a rAAV.flex-eGFP (Fig. 2C) led to labeling of less than half as many neurons (Fig. 2D).

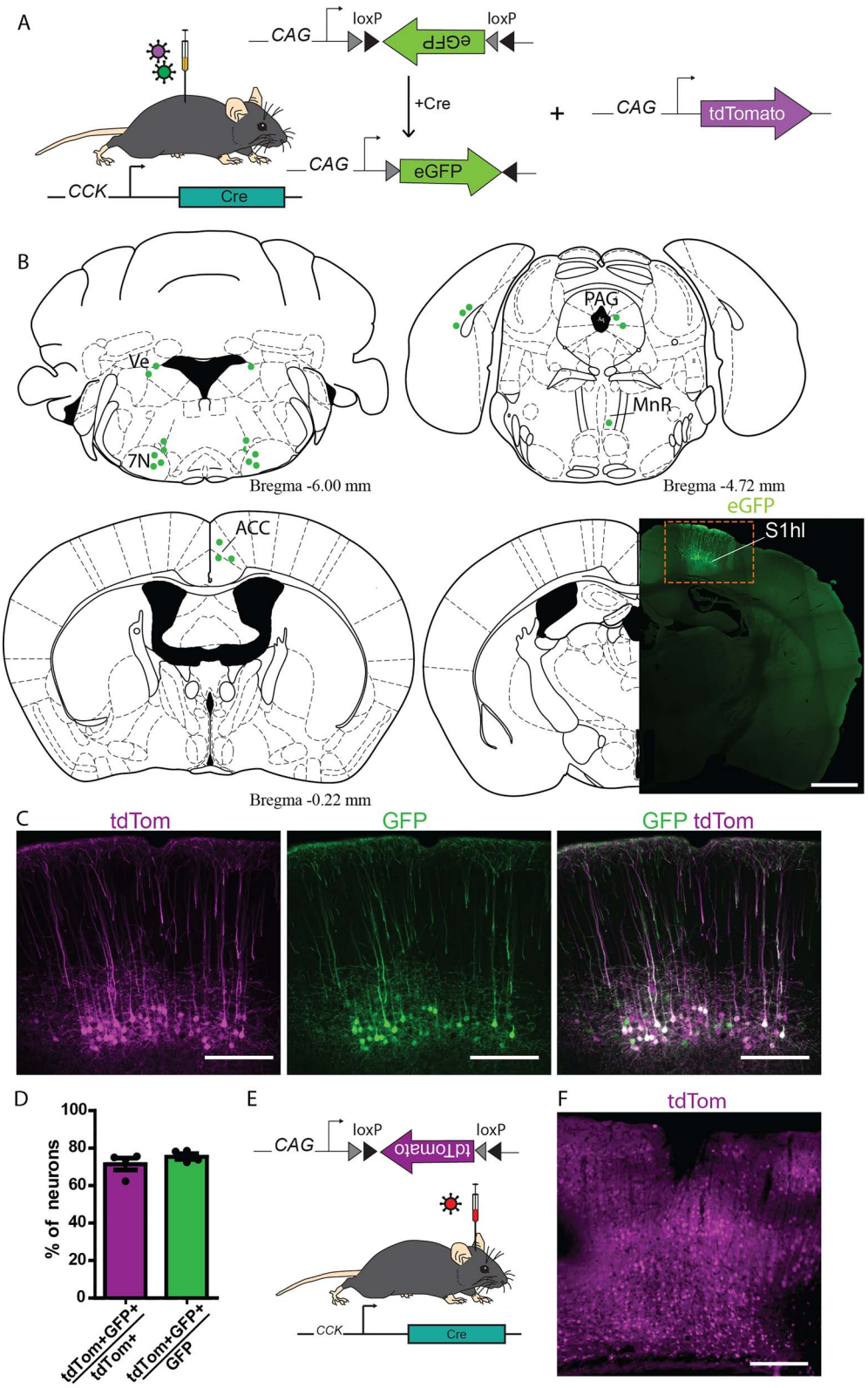

Figure 1. Labeling S1-CST neurons in CCK^{Cre} mice. (*A*) Injection of rAAVs encoding for Cre-dependent eGFP and Cre-independent tdTomato fluorescent proteins into the lumbar spinal cord of CCK^{Cre} mice ($n = 4$ mice). (*B*) Brain areas labeled with eGFP positive neurons after intraspinal injection of rAAV2retro.flex.eGFP in CCK^{Cre} mice. 7N: facial nuclei, ACC: anterior cingulate cortex, MnR: median raphe nucleus, PAG: Periaqueductal gray, S1hl: somatosensory cortex, hindlimb area. (*C*) Comparison of S1-CST neurons labeled by Cre-dependent eGFP and Cre-independent tdTomato ($n = 4$, 3166 neurons) fluorescent proteins. (*D*) Quantification of (*C*). (*E*) Injection of rAAVs encoding for Cre-dependent tdTomato into the S1 cortex of CCK^{Cre} mice. (*F*) Widespread labeling of cortical neurons with tdTomato (red) after cortical injection (*E*). Error bars represent ±SEM. Scale bars: *B*: 1 mm; *C* and *F*: 200 µm.

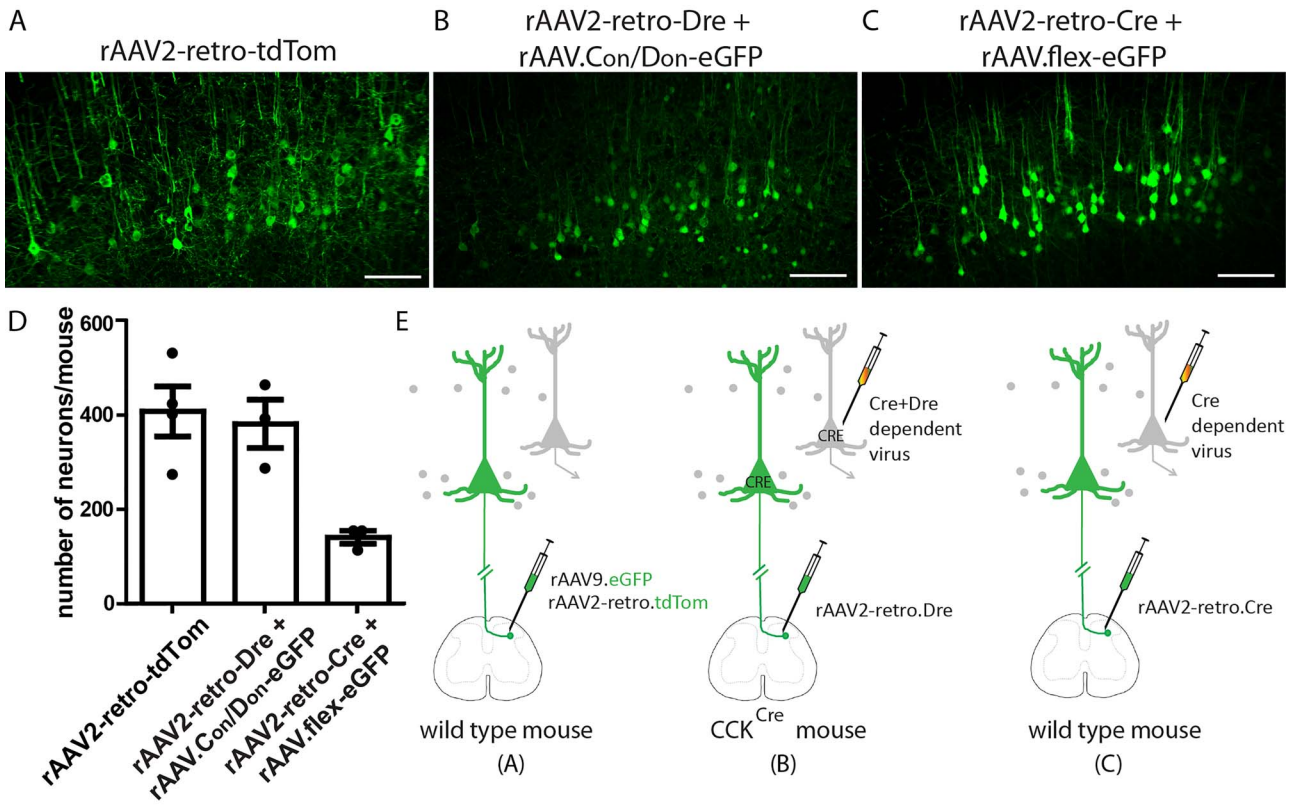

Figure 2. Three viral targeting strategies to label S1-CST neurons. (*A*) S1-CST neurons labeling using a rAAV2-retro-tdTomato injected in the lumbar spinal cord of wild-type mice. (*B*) S1-CST neurons labeling using the rAAV2-retro-Dre injected in the lumbar spinal cord of CCK^{Cre} mice, followed by cortical (S1) injection of $AAV.C_{ON}/D_{ON}$-eGFP. (*C*) S1-CST neurons labeling using the rAAV2-retro-Cre injected in the lumbar spinal cord of wild-type mice, followed by cortical (S1) injection of AAV.flex-eGFP. (*D*) Quantification of the number of neurons labeled per mouse in (*A*–*C*) (*A*: $n = 4$ mice, 1546 neurons; B: $n = 3$ mice, 1136 neurons and *C*: $n = 3$ mice, 418 neurons). (*E*) Diagrams showing the 3 injections strategies used in (*A*), (*B*), and (*C*), respectively. Error bars represent: ±SEM. Scale bars: 100 µm.

Molecular Characterization of S1-CST Neurons

Since virtually all S1-CST neurons projecting to the lumbar spinal cord express CCK, we next asked whether these neurons constitute a homogeneous population or are assembled from different subpopulations. To this end, we injected a rAAV2-retro.flex.eGFP into the spinal cord of CCK^{Cre} mice and performed multiplex ISH against several established markers for cortical neurons in cortex sections obtained from the virus-injected mice (Fig. 3A–E). Consistent with our initial characterization of the CCK^{Cre} mice, we found that all eGFP-labeled neurons expressed the CCK mRNA (Fig. 3A). Furthermore, the vast majority of eGFP labeled CST-neurons expressed well-established marker genes of cortical layer 5 neurons (Arlotta et al. 2005; Molyneaux et al. 2007; Watakabe et al. 2007; Klingler et al. 2019) including *Crhr1* (78.9 ± 4.9%), Er81 (79.2 ± 6.5%), or *Ctip2* (80.8 ± 2.5%) (Fig. 3A–C, respectively). We also found that 48.2 ± 4.0% of $eGFP^+$ neurons expressed *RORα* and 23.5 ± 1.4% expressed *Nurr1* (Fig. 3D) mRNAs, indicating molecular heterogeneity within the CCK^+ CST neurons. Expression of several other genes was detected at low levels and only in few $eGFP^+$ neurons (*gabrg1*: 12.8 ± 2.3%, *5HT2c*: 10.37 ± 3.6%, and *Plxnd1*: 4.33 ± 1.4%, Fig. 3D,E, RNAscope negative probe background level is depicted in Supplementary Fig. 4).

Morphology of S1-CST Neurons

We next examined whether S1-CST neurons send collaterals to other CNS regions before they reach the spinal cord. We employed the intersectional strategy described above to label CCK^{Cre} S1-CST neurons (Fig. 2B). Three weeks after the virus injections, entire mouse CNS were dissected and cleared using the passive CLARITY procedure (Chung et al. 2013). Cleared entire mouse CNS were imaged with light-sheet microscopy (Voigt et al. 2019). The vast majority of S1-CST neuron axons ran from the cortex through the internal capsule and to the midbrain pyramids, following the known trajectory of the main CST (Fig. 4) (Wang et al. 2017). In addition, we detected a few collaterals branching from the main tract at 2 sites: a small number of axons bifurcated from the internal capsule to terminate in the dorsal striatum (Fig. 4B,C), and another small group branched-off in the midbrain innervating posterior thalamic nuclei (Fig. 4D) and tectal areas (Supplementary Fig. 5D,E). The latter is consistent with observations from Wang et al. in the motor cortex-derived CST (Wang et al. 2017). As expected, the CST axons travel from a ventral to a dorsal location as they leave the brainstem to enter the spinal cord. At this level the tract is also moving to the contralateral side of the spinal cord (pyramidal decussation, Fig. 4E). We observed a few axons branching into the dorsolateral CST (Fig. 4E–G,I,J) (Steward et al. 2004; Kathe et al. 2014). In the lumbar spinal cord, axons bifurcate from the CST into the dorsal horn gray matter (corresponding to the location of their spinal targets and the site of injection of the Dre carrying virus). We did not observe collaterals into segments of the spinal cord other than the lumbar segments (Fig. 4H,K).

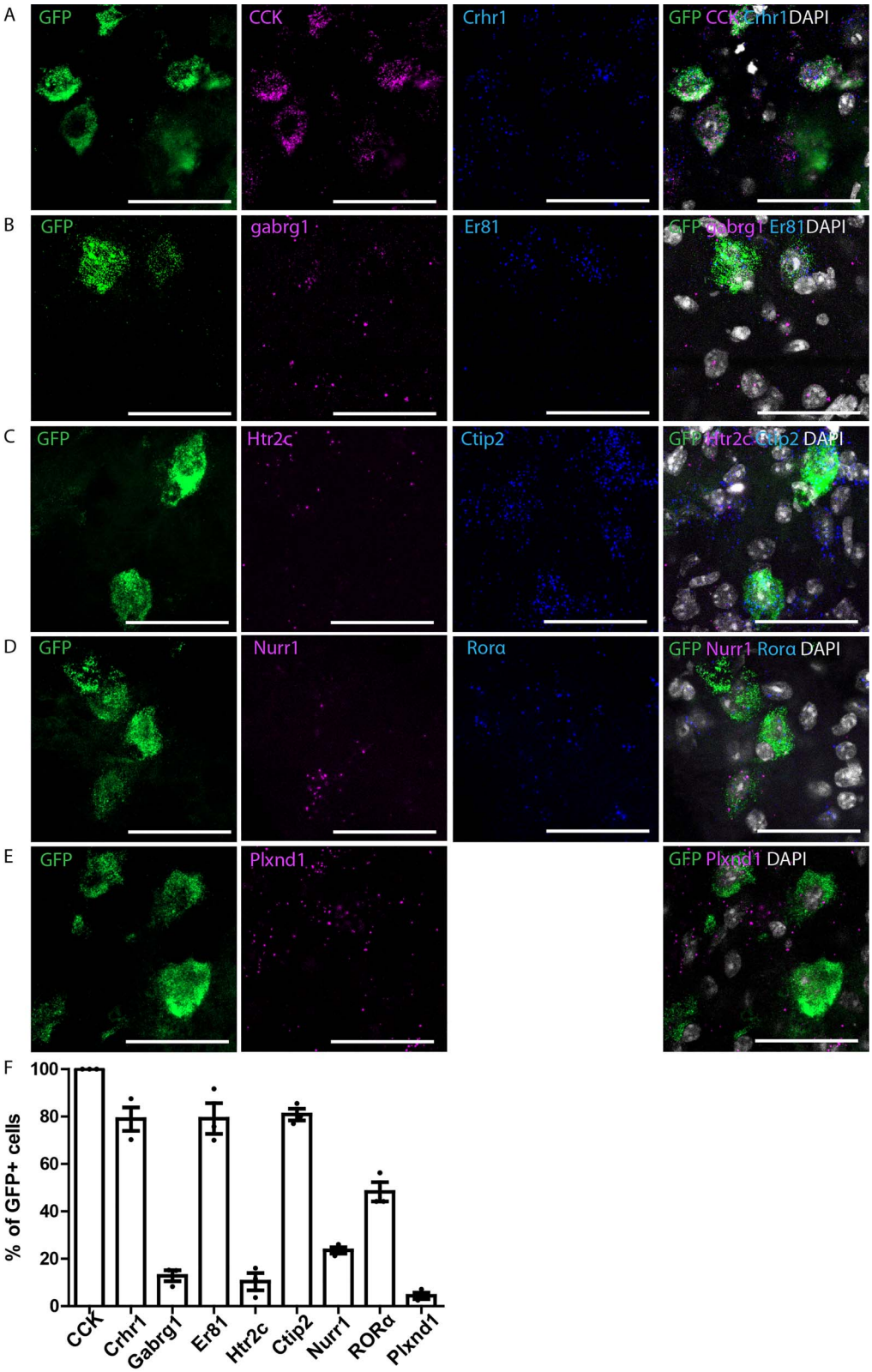

Figure 3. Multiplex ISH in GFP-labeled CCK^{Cre} neurons with cortical neurons markers in S1. (*A–E*) Triple ISH showing the colocalization of GFP with *CCK* and *crhr1* (*A*), *gabrg1* and *er81* (*B*), *htrc2* and *ctip2* (*C*), nurr1 and *RORα* (*D*), *Plxnd1* (*E*). (*F*) Quantification of (*A–E*) ($n = 3$ mice; 352, 221, 85, 243, and 278 GFP neurons, respectively). Error bars represent ±SEM. Scale bars: 50 μm.

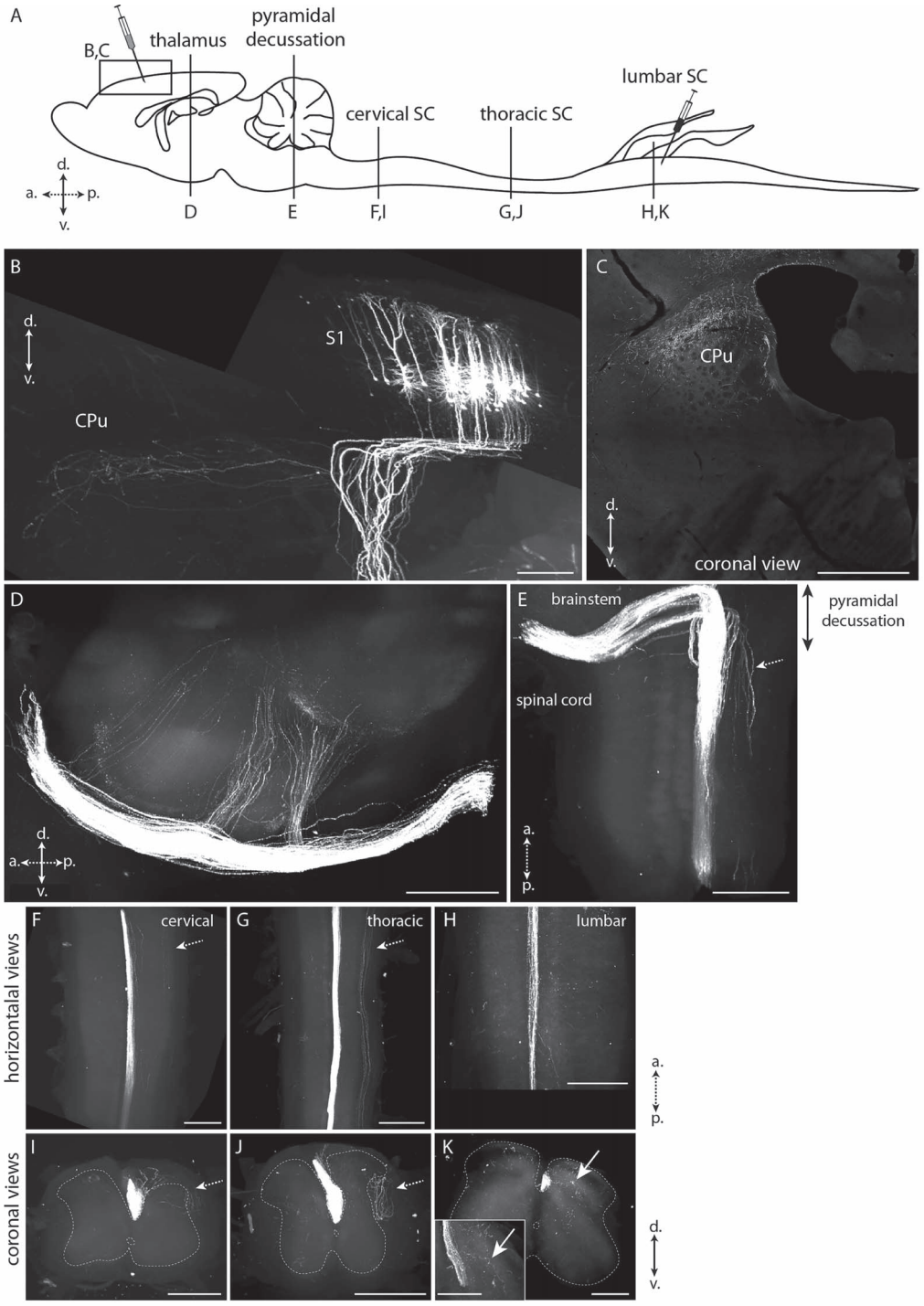

Figure 4. Labeling of the corticospinal tract in CLARITY-cleared brain. The whole CNS of mice expressing eGFP only in lumbar spinal cord projecting CST neurons was dissected and subjected to passive clearing and light sheet imaging. (*A*) Schematic drawing of the mouse CNS. Injection sites of the viruses and optical planes shown in *B*–*K* are depicted. (*B*) eGFP labeling of S1-CST neurons in S1. The axons enter the corpus callosum and a small subset of collaterals bifurcates to the dorsal striatum (CPu). (*C*) Coronal view of the termination area in the CPu. (*D*) Sagittal view of collaterals branching of from the main CST towards the thalamus. (*E*) Horizontal view of the CST decussation at the entry of the spinal cord. (*F*,*I*) Horizontal and coronal views of the CST at the level of the cervical spinal cord. (*G*,*J*) Horizontal and coronal views of the CST at the level of the thoracic spinal cord. (*H*,*K*) Horizontal and coronal views of the CST at the level of the lumbar spinal cord. Inset in (*K*) shows CST terminals branching in the dorsal horn. White arrows: CST terminals branching in the spinal cord at the lumbar level only. Dashed arrows: dorsolateral tract (secondary part of the CST). CPu: Striatum; S1: primary somatosensory cortex (hindlimb area here); SC: spinal cord; a.: anterior, p.: posterior, d.: dorsal, v.: ventral. *B*, *D*–*K*: Volume renderings (Imaris); *C*: optical section. ($n = 3$ mice). Scale bars: 1 mm.

S1-CST Neurons Receive Input from the Somatosensory Circuit

The direct connection between the spinal dorsal horn and the somatosensory cortex suggests that S1-CST neurons may be part of a circuit for sensory processing. We therefore further investigated the precise position of S1-CST neurons in this circuit by tracing their presynaptic input and postsynaptic target neurons. We started with the identification of neurons presynaptic to S1-CST neurons and performed monosynaptic retrograde labeling using genetically engineered rabies virus (Callaway and Luo 2015). In order to label as many neurons as possible (Fig. 2D), S1-CST neurons were targeted in CCK^{Cre} mice by intraspinal injection of rAAV2-retro.Dre followed by local injection of a Cre and Dre dependent helper virus (rAAV.flex.rox.TVA.SAD19-G) into the primary somatosensory cortex S1 (Fig. 5). The helper virus provided the TVA (Tva receptor) gene for selective infection by EnvA-pseudotyped rabies virus and the rabies glycoprotein (SAD19-G) for trans-complementation enabling retrograde labeling across one synapse. We then injected a glycoprotein-deficient EnvA-pseudotyped rabies virus (EnvA.RV.ΔG.eGFP) into the S1 cortex. We found that eGFP was expressed in layer 5 pyramidal neurons (including the primarily infected S1-CST neurons, Fig. 5A and Supplementary Fig. 6) and in many pyramidal neurons of layer 2/3 (Fig. 5E,F). In layer 5, the rabies virus also labeled interneurons that expressed PV (15.4 ± 2.73% of GFP^+TVA^- neurons), and rarely somatostatin (SST; 0.77 ± 0.41%) or NPY (0.74 ± 0.74%) (Fig. 5G–I), 3 well-characterized markers of cortical inhibitory interneurons (Xu et al. 2010), representing approximatively 60–70% of cortical inhibitory interneurons (Gonchar et al. 2007).

We also found $eGFP^+$ neurons in the VPL nucleus of the thalamus (Fig. 5C,D, 10.9 ± 4.8% of GFP^+TVA^- neurons). The morphology of these cells resembled that of previously described thalamocortical sensory relay neurons (Tlamsa and Brumberg 2010). This connectivity pattern is hence similar to what has previously been described for CST neurons in other studies (Abraira and Ginty 2013; Constantinople and Bruno 2013; McMahon et al. 2013). Our results thus demonstrated that CCK-expressing S1-CST neurons are part of a direct sensory circuit loop between the spinal cord, thalamic nuclei and the somatosensory cortex.

Labeling of CST Axons in the Spinal Cord

The termination area of S1-CST neurons in the lumbar spinal cord (Fig. 6) was studied after injection of rAAV1.flex.tdTomato in the somatosensory cortex hindlimb area (S1hl) of CCK^{Cre} mice. Labeled CST axons were mainly found in the ventral part of the spinal dorsal funiculus (Fig. 6A, "CST"). Terminals were also visible within the gray matter of the deep dorsal horn (laminae III and IV) (Fig. 6A and Supplementary Fig. 7B,C). This finding is consistent with previous reports showing that tracing from the motor cortex labeled terminals mainly in the ventral and intermediate spinal cord, whereas tracing from S1 labeled terminals in laminae III and IV of the dorsal horn (Kamiyama et al. 2015; Wang et al. 2017; Ueno et al. 2018). These dorsal horn laminae constitute the termination area of low-threshold mechanoreceptive fibers (Abraira et al. 2017). In addition, they contain interneurons which process touch and proprioceptive information, and have been shown to be critically involved in abnormal somatosensory processing in neuropathic pain (Foster et al. 2015; Peirs et al. 2015; Petitjean et al. 2015; Cheng et al. 2017). We therefore decided to identify the spinal neurons that are targeted by S1-CST neurons in this region.

Anterograde Transsynaptic Tracing with Wheat Germ Agglutinin

We used wheat germ agglutinin (WGA) to label neurons that are targeted by S1-CST neurons. CCK^{Cre} mice were injected with rAAV2.flex.WGA into S1hl. WGA is transported transsynaptically to label postsynaptic neurons (Braz et al. 2002). After 10 days, we detected WGA in the dorsal horn of the lumbar spinal cord (Fig. 6C–F). As expected, WGA immunoreactivity was mostly found in the deep dorsal horn laminae III and IV (Fig. 6C–F and Supplementary Fig. 7B,C). In order to identify the neurons labeled with WGA, we stained sections with antibodies against known markers of different dorsal horn interneuron populations. We found that about one-third of the WGA labeled neurons were positive for Lmx1β (33.5 ± 1.4%), which is expressed by most excitatory interneurons in laminae I–III (Del Barrio et al. 2013; Albisetti et al. 2019) (Fig. 6B,C). More than half of the labeled neurons (56.9 ± 2.1%) were positive for Pax2, a marker of dorsal horn inhibitory neurons (Del Barrio et al. 2013; Albisetti et al. 2019) (Fig. 6B,D). When performing anterograde tracing in animals crossed to GlyT2::eGFP mice, a little less than half of all WGA positive dorsal horn neurons (45.8 ± 2.8%, Fig. 6B,E) were $eGFP^+$ indicating that they were glycinergic (Jursky and Nelson 1995; Poyatos et al. 1997; Spike et al. 1997; Zeilhofer et al. 2005). Notably, we found that more than half of all WGA positive neurons also expressed the transcription factor c-Maf (54.8 ± 3.9%; Fig. 6B,F), which is required for the proper development of laminae III/IV interneurons (Hu et al. 2012). Because c-Maf is present in both excitatory and inhibitory dorsal horn interneurons (Hu et al. 2012; Del Barrio et al. 2013), we determined the portion of WGA and c-Maf double-positive neurons that were either inhibitory (Pax2 positive: 21.9 ± 2.6% of all WGA^+ neurons) or excitatory (Pax2 negative: 27.5 ± 1.9% of all WGA^+ neurons). We did not find any WGA positive neurons that were also positive for protein kinase Cγ (PKCγ), a marker of a small subpopulation of excitatory dorsal horn neurons located at the border between laminae II and III (Malmberg et al. 1997; Polgar et al. 1999). WGA is an anterograde tracer that can cross multiple synapses. We have limited the incubation time after injection of the rAAV2.flex.WGA to obtain mostly monosynaptic labeling. However, to verify that the majority of WGA labeled spinal neurons received direct inputs from CST neurons, we coinjected viruses carrying a transgene for WGA (rAAV2.flex.WGA) together with a rAAV carrying a transgene encoding a synaptophysin-eGFP fusion-protein into the S1hl. We found that 89.6 ± 6.3% of WGA^+ neurons showed at least one GFP^+ apposition close to a homer labeled postsynapse on the cell body (Fig. 6G,H and Supplementary Fig. 7D,E) demonstrating that the vast majority of WGA labeled spinal neurons receive monosynaptic input from CST neurons in S1. In agreement with the absence of WGA labeled PKCγ neurons, we found GFP^+ contacts on only 6.37 ± 2.7% of PKCγ positive neurons (Supplementary Fig. 7F). Our results therefore suggest that S1-CST neurons contact a rather heterogeneous population of interneurons in the dorsal horn, including glycinergic neurons and c-Maf expressing neurons.

Discussion

In the present study, we developed intersectional rAAV-based strategies to characterize S1-CST neurons that innervate the spinal cord. We found that these neurons constitute a genetically heterogeneous group of neurons that in turn innervate a heterogeneous target population in the spinal dorsal horn. Furthermore, we show that they receive direct input from sensory

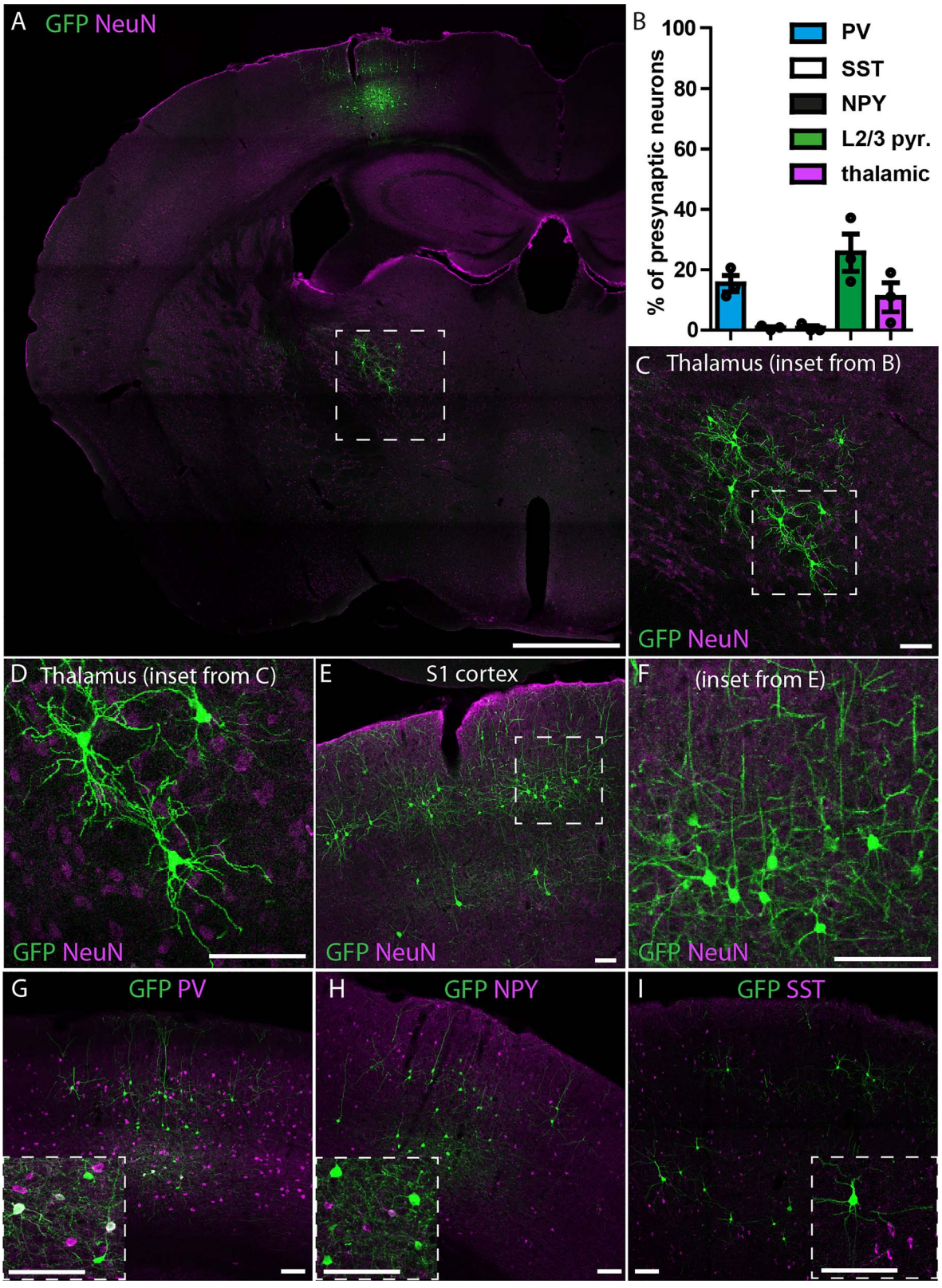

Figure 5. Retrograde monosynaptic tracing of S1-CST neurons with rabies. rAAV2retro.Dre was injected into the spinal cord of CCK^{Cre} mice, followed by a Cre-and-Dre-dependent helper virus (TVA, RabG) into S1. Two weeks later the pseudotyped rabies virus was injected into S1. (*A*) Overview of the labeled neurons in the brain: S1-CST neurons (starter cells) as well as layer 2/3 pyramidal neurons, thalamic sensory relay neurons, and layer 5 inhibitory interneurons. (*B*) Quantification of retrogradely labeled neurons (GFP^+TVA^-) represented in (*C*–*I*). (*C*,*D*) Retrogradely labeled thalamic sensory relay neurons in the VPL of the thalamus ($n = 3$ mice, 1481 GFP^+ neurons). (*E*,*F*) Retrogradely labeled layer 2/3 pyramidal neurons ($n = 3$ mice, 1481 GFP^+ neurons). (*G*–*I*) Retrogradely labeled layer 5 inhibitory interneurons, with costaining against PV (*G*, $n = 3$ mice, 513 neurons), NPY (*H*, $n = 3$ mice, 196 GFP^+ neurons) or SST (*I*, $n = 3$ mice, 968 GFP^+ neurons). Error bars represent ±SEM. Scale bars: *A*: 1 mm; *C*–*I*: 100 µm.

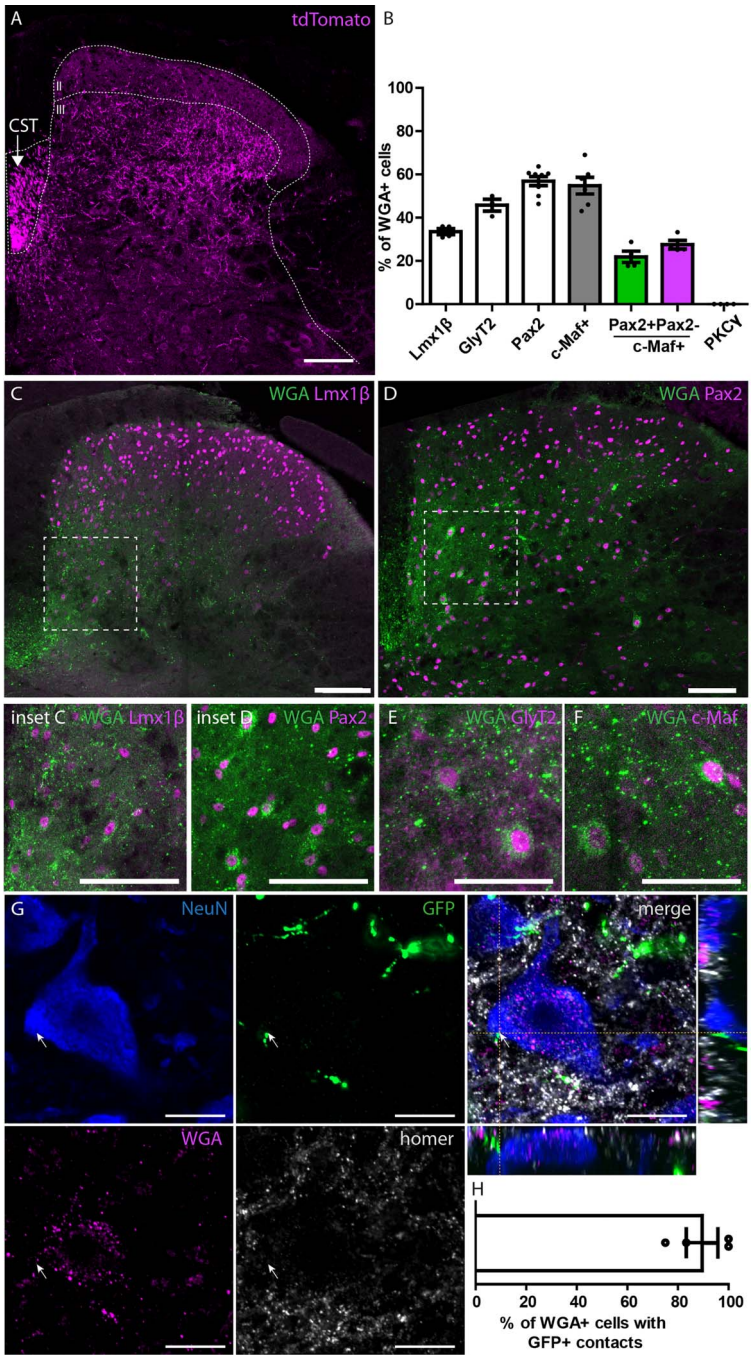

Figure 6. Labeling of the output of S1-CST neurons in the spinal cord. (*A*) Labeling of the CST in the dorsal funiculus of the spinal cord, contralateral to the brain injection site after injection of a rAAV carrying a Cre-dependent tdTomato into S1hl of CCK^{Cre} mice. CST terminals are preferentially located below the laminae II-III border ($n = 3$). (*B*) Quantification of the number of WGA positive neurons after injection of a rAAV.flex.WGA into S1hl of CCK^{Cre} mice. Quantified are WGA positive neurons that express Lmx1β ($n = 4$, 320 WGA^+ neurons), Pax2 ($n = 8$, 391 WGA^+ neurons), GlyT2 ($n = 3$, 275 WGA^+ neurons), c-Maf ($n = 6$, 506 WGA^+ neurons), or PKCγ ($n = 4$, 201 WGA^+ neurons). (*C*,*D*) Representative images of colabeled WGA positive neurons in the spinal cord with the excitatory marker Lmx1β ((*C*) and inset) and the inhibitory marker Pax2 ((*D*) and inset). Neurons expressing eGFP under the GlyT2 promoter (using the GlyT2::eGFP mouse line (*E*)), and neurons expressing the transcription factor c-Maf (*F*) were also found positive for WGA. (*G*,*H*) Verification of monosynaptic labeling by WGA. CCK^{Cre} Mice were coinjected with rAAV.flex.WGA and rAAV.flex.Syp-eGFP (encoding a Cre-dependant synaptophysin-eGFP fusion protein) into S1hl. (*G*) Colabeling of WGA positive neurons in the spinal cord with the neuronal marker NeuN and eGFP labeled presynaptic terminals of S1-CST neurons. Depicted is a representative example of a WGA^+ neuron in close proximity to a $eGFP^+$ presynaptic terminal of a S1-CST neuron3. (*H*) Quantification of the number of WGA^+ neurons receiving direct contacts from $eGFP^+$ synaptic terminals ($n = 4$ mice; 25 neurons). CST: corticospinal tract. Error bars represent ±SEM, Scale bars: *A* and *C*–*F*: 100 µm; *G*: 10 µm.

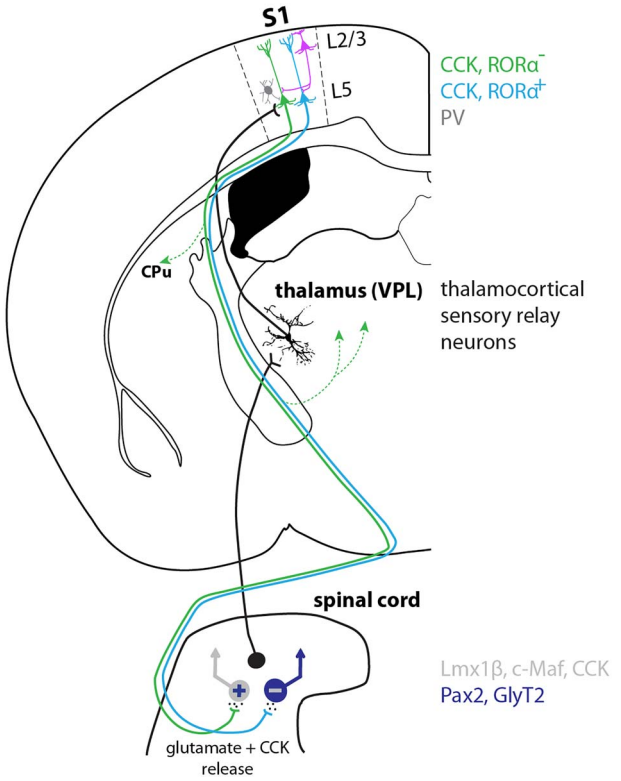

Figure 7. Model of a spinothalamocortical feedback circuit. Spinal projection neurons relay sensory information to the VPL nucleus of the thalamus. Sensory thalamocortical relay neurons propagate the information directly to CST neurons in S1. S1-CST neurons also receive direct synaptic input from inhibitory (PV) neurons and pyramidal layer 2/3 neurons. S1-CST neurons do not only innervate the spinal cord but also send collaterals to the dorsal striatum (CPu) as well as thalamic nuclei (indicated by dotted green lines with arrow). We speculate that different subpopulations of CST neurons (e.g., RORα$^+$ or RORα$^-$) project back onto different types of spinal interneurons (e.g., inhibitory [GlyT2$^+$, Pax2$^+$] or excitatory [Lmx1β$^+$, CCK$^+$, c-Maf$^+$]) and thus exert potentially modality specific functions (see Discussion). CST neurons likely modulate spinal target neurons through release of glutamate as well as the neuropeptide CCK.

thalamic relay neurons in addition to intracortical synaptic input from layer 2/3 pyramidal and from PV positive interneurons. These results establish a long-range feedback loop between the sensory spinal cord and the output neurons of the primary somatosensory cortex (Fig. 7).

CCK Expression in S1-CST Neurons

We found that the majority of S1-CST neurons expressed mRNA encoding for the neuropeptide CCK. CCK expression in CST neurons suggests that they do not only release glutamate but likely also release CCK, which may modulate processing at the spinal level. CCK activates 2 distinct receptors (CCK-A and CCK-B) that are both expressed in the adult rodent spinal cord (Lein et al. 2007; Kim et al. 2009; Haring et al. 2018). In particular, CCK-B has been reported to exert antagonizing effects on morphine-induced analgesia (Wiesenfeld-Hallin et al. 1999; Coudore-Civiale et al. 2000; Kovelowski et al. 2000; Wiesenfeld-Hallin et al. 2002). However, CCK release has also been linked to antinociceptive effects (Roca-Lapirot et al. 2019). At the level of the spinal cord, CCK is released from multiple sources, including local CCK neurons (Haring et al. 2018), and probably from supraspinal sites (e.g., S1, anterior cingulate cortex, the thalamus, and the RVM; Fig. 1). The release from different sites may contribute to the opposing effects or facilitate effects mediated by CCK.

Molecular Heterogeneity of S1-CST Neurons

The results presented in this study suggest that S1-CST neurons are not a homogenous set of neurons but can be subdivided into subsets of neurons that differ in their molecular signature, as is the case for other projection neurons (Gerfen et al. 2013; Kim et al. 2015; Xu 2020). The great majority, perhaps even all, of CST neurons in S1 express CCK, in addition to other well-established markers of cortical layer 5 neurons such as Ctip2 and ER81 (Arlotta et al. 2005; Molyneaux et al. 2007). Additionally, other genes such as the nuclear receptors *RORα* (48.2%) or *Nurr1* (23.5%) are only expressed in subsets of CCK$^+$ CST neurons. RORα and Nurr1 are nuclear receptors capable of driving specific transcriptional programs, suggesting that the subpopulations marked by the expression of the respective genes can be distinguished by a number of molecular markers. Until recently projection neurons within a cortical layer were considered as a rather homogenous population. However, in line with our findings recent RNAseq single cell data suggest a heterogeneous composition that is at least in part dependent on the target area (Xu 2020). Our data suggest that even cortical projection neurons that target the same CNS area (i.e., the lumbar dorsal horn of the spinal cord) are molecularly heterogeneous. It is possible that this molecular heterogeneity translates into a functional heterogeneity of S1-CST neurons, comparable with what has been observed for other populations of cortical output neurons (Kim et al. 2015; Klingler et al. 2019).

Presynaptic Input to S1-CST Neurons

In contrast to previous studies, we specifically targeted lumbar spinal cord projecting CST neurons in S1, thus enabling circuit analysis at an unprecedented resolution. Taking advantage of this, we were able to conduct retrograde monosynaptic tracing with rabies virus. Our experiments revealed that S1-CST neurons receive direct intracortical input from layer 2/3 pyramidal neurons as well as from inhibitory PV and to a lesser extend from NPY and SST interneurons. Contrary to what has been suggested by previous studies (Tanaka et al. 2011; Cichon et al. 2017), we found only little input from SST interneurons. We see 2 possible explanations: first, the previous studies did not directly address direct connections between SST neurons and specifically CST neurons in layer 5 of S1 and it is possible that different subsets of layer 5 pyramidal neurons receive distinct patterns of input (Anderson et al. 2010; Xu 2020). Second, we have previously shown that rabies-based retrograde transsynaptic tracing can be biased and does not always detect all inputs (Albisetti et al. 2017). We also identified direct input from sensory relay neurons in the VPL of the thalamus. This nucleus receives input from the postsynaptic dorsal column, the direct dorsal column pathway and the spinocervical tract that are known to propagate tactile information from the periphery to the brain (Abraira and Ginty 2013). Our data therefore indicate that CST neurons in S1 integrate direct ascending spino-thalamic sensory information with intra cortical input from layer 2/3 pyramidal neurons and local input from inhibitory interneurons. This is in agreement with the long-held view that sensory information relayed via the thalamus to the cortex is preprocessed by propagation from cortical layer 4 to layer 2/3 neurons, before arriving at the main output neurons of the somatosensory cortex located in the layer 5 (Gilbert and Wiesel 1979; Harris and Shepherd 2015). Moreover,

it is also in agreement with in vivo evidence indicating the existence of direct connections between the thalamus and layer 5 neurons (Constantinople and Bruno 2013). The authors of the latter study suggested however that intracortical input might not be necessary for sensory evoked activity in layer 5 neurons. Bridging these opposing views, Quiquempoix et al. (2018) provided evidence that layer 2/3 pyramidal neurons primarily play a major role in tuning/amplifying sensory evoked responses in cortical output neurons of layer 5. Our data suggest that this model probably applies to CST neurons in layer 5 of S1.

Non Spinal Target Sites of CST Neurons

When analyzing the output of S1-CST neurons, we found evidence that, although they mainly project through the CST onto the spinal dorsal horn, they also send collateral branches to the dorsal striatum and thalamic nuclei and tectal areas. This extends, confirms and further specifies previous experiments in which CST collaterals were observed when all spinally projecting neurons were labeled (Wang et al. 2017; Wang et al. 2018). Our data therefore indicate that, while their main target is the spinal dorsal horn (Ueno et al. 2018), S1-CST neurons also contribute to cortico-striatal projections and may thereby influence goal-directed behaviors (Wang et al. 2017). In addition, collaterals in the posterior thalamic nuclei are likely to influence thalamic integration of sensory inputs, possibly to adjust cortical responses to predicted versus unpredicted sensory signals (Groh et al. 2014; Casas-Torremocha et al. 2017).

Spinal Target Neurons and Functional Implications on Nociceptive Signaling

Our anterograde tracing experiments revealed that CCK$^+$ S1-CST neurons target different populations of spinal interneurons, with excitatory and inhibitory phenotypes being about equally prevalent among dorsal horn S1-CST target neurons. These results are also in line with findings from Ueno et al., who showed that S1 and M1-derived CST neurons contact distinct populations of spinal interneurons (Ueno et al. 2018). In addition, they provided evidence that the spinal neurons targeted by S1-CST neurons are involved in skilled movements. In another recent study, Liu et al. (2018) observed changes in light touch sensitivity after ablation or silencing of S1-CST neurons in naïve and neuropathic states and proposed a neuropathic pain promoting role of S1-CST neurons. We found that a large portion of the inhibitory target neurons were glycinergic neurons and the majority of the excitatory neurons expressed c-Maf, a transcription factor necessary for the development of deep dorsal horn interneurons (Hu et al. 2012). We have previously demonstrated that glycinergic dorsal horn neurons are an integral part of the spinal gate that controls spinal pain and itch relay (Foster et al. 2015) and that activation of these neurons exerts a strong analgesic effect. Conversely, deep dorsal horn excitatory neurons have been linked not only to fine motor control (Bourane et al. 2015; Ueno et al. 2018) but also to chronic pain states (Peirs et al. 2015; Cheng et al. 2017; Liu et al. 2018). The c-Maf$^+$ neurons identified in the present study are likely a subset of dorsal horn CCK$^+$ excitatory interneurons (Haring et al. 2018) and CST-mediated activation of CCK$^+$ spinal interneurons has strongly been linked to chronic pain states (Liu et al. 2018). Interestingly, we found little direct input of S1 CST neurons onto PKCγ neurons. A previous study has suggested that most PKCγ neurons receive cortical input (Abraira et al. 2017). However, in that study, projection neurons and projection neuron terminals descending from the brain to the spinal cord have been labeled by crossing the Emx1^{Cre} driver line to the Ai34 reporter line (R26$^{synaptophysin\text{-}tdTomato}$). Emx1^{Cre} mediated recombination has been reported to occur predominantly in excitatory neurons of the dorsal pallium, including the AAC, which also projects to the lumbar spinal dorsal horn (Fig. 1*B* and Supplementary Fig. 2*D*). In addition, significant recombination has also been observed in the claustrum and in the basomedial and lateral nuclei of the amygdala (Gorski et al. 2002). Taken together, these findings suggest that most of the descending input to spinal PKCγ neurons does not originate from S1.

Like CCK neurons PKCγ neurons have also been strongly linked to neuropathic pain symptoms (Malmberg et al. 1997; Martin et al. 2001), and they are also a subset of CCK$^+$ spinal interneurons albeit different from the c-Maf$^+$ interneurons. Our results therefore suggest that CST neurons could promote chronic pain states via engaging the c-Maf$^+$ subset of CCK$^+$ spinal interneurons. Conversely, it is likely that CST neurons can also have an analgesic function by stimulating deep dorsal horn glycinergic neurons.

Outlook—Intersectional Targeting of CST Neurons

Most studies of the CST focused on its input to the ventral horn, its function in fine motor control (Wang et al. 2017; Ueno et al. 2018; Wang et al. 2018), and its role in the generation of deficits after spinal cord injury and their recovery (Steward et al. 2008; Fry et al. 2010; Jin et al. 2015). Our data and the study by Liu et al. (2018) indicate that S1-CST target neurons also play a role in nociceptive signaling. Activation of all CST neurons in optogenetic or chemogenetic experiments would activate both inhibitory and excitatory spinal interneurons with potentially opposing effects on nociceptive signaling. Although unproven, it is well possible that different subtypes of spinal S1-CST target neurons (such as excitatory and inhibitory spinal interneurons) are innervated by distinct subsets of S1-CST neurons. We have shown that CST neurons in S1 are not a homogenous population. The intersectional targeting strategies presented here allow further dissecting of the function of potential CST subpopulations. For example, applying the same intersectional targeting strategies to RORα^{Cre} mice will uncover which neuronal subtypes are targeted by the RORα^+ subset.

Alternatively, retrograde tracing initiated at the level of a specific spinal target populations identified by us and others (Abraira et al. 2017; Ueno et al. 2018) may be used in order to identify target-specific subnetworks and functionally interrogate subpopulations of S1-CST neurons. Self-inactivating rabies virus such as those recently developed by Ciabatti et al. (2017) may be suitable to functionally manipulate the S1-CST neuron population that innervates the respective spinal target populations. Finally, our study highlights the importance of spatially restricted and intersectional manipulation of either CST or spinal neurons that express a given marker gene, as several of the genes that we and others found expressed in CST neurons are also present in spinal cord neurons (e.g., *CCK*, *RORα*, or *Pkcγ*).

Supplementary Material

Supplementary material can be found at *Cerebral Cortex Communications* online.

Notes

We want to thank Jean-Charles Paterna (Viral Vector Facility, UZH, Zurich, Switzerland) for the production of viral vectors. N.F. carried out the experiments, E.P., J.M.M., U.Z., R.K., T.K., F.H., and F.F.V. contributed to the CLARITY experiments and helped with the analysis. N.F., H.W, and H.U.Z. wrote the manuscript. H.W. and H.U.Z. supervised the project. All authors have read and commented on the manuscript. *Conflict of Interest:* None declared.

Funding

The Clinical Research Priority Program of the University of Zurich ("Pain–From phenotype of mechanisms" to H.U.Z.); a Contrat Doctoral Specifique pour Normaliens (CDSN) grant awarded for a joint PhD at the University of Zürich and the Institute of Biology of the École Normale Supérieure (IBENS), Paris Sciences et Lettres Research University (PSL), Paris 75005, France (to N.F.); the Technology Platform commission of the University of Zürich (to E.P.); an European Research Council (ERC) (advanced grant project no. 670757 to F.H.); the European Research Council (679175, T.K.); the Swiss National Science Foundation (SNSF) (310030B_176398 to H.U.Z. and 31003A_170037, T.K.); the Swiss Foundation for Excellence in Biomedical Research (to R.K. and T.K.).

References

Abraira VE, Ginty DD. 2013. The sensory neurons of touch. *Neuron*. **79**:618–639.

Abraira VE, Kuehn ED, Chirila AM, Springel MW, Toliver AA, Zimmerman AL, Orefice LL, Boyle KA, Bai L, Song BJ, et al. 2017. The cellular and synaptic architecture of the mechanosensory dorsal horn. *Cell*. **168**:295–310 e219.

Albisetti GW, Ghanem A, Foster E, Conzelmann KK, Zeilhofer HU, Wildner H. 2017. Identification of two classes of somatosensory neurons that display resistance to retrograde infection by rabies virus. *J Neurosci Res*. **37**:10358–10371.

Albisetti GW, Pagani M, Platonova E, Hosli L, Johannssen HC, Fritschy JM, Wildner H, Zeilhofer HU. 2019. Dorsal horn gastrin-releasing peptide expressing neurons transmit spinal itch but not pain signals. *J Neurosci Res*. **39**:2238–2250.

Anderson CT, Sheets PL, Kiritani T, Shepherd GM. 2010. Sublayer-specific microcircuits of corticospinal and corticostriatal neurons in motor cortex. *Nat Neurosci*. **13**:739–744.

Arlotta P, Molyneaux BJ, Chen J, Inoue J, Kominami R, Macklis JD. 2005. Neuronal subtype-specific genes that control corticospinal motor neuron development in vivo. *Neuron*. **45**:207–221.

Bareyre FM, Kerschensteiner M, Misgeld T, Sanes JR. 2005. Transgenic labeling of the corticospinal tract for monitoring axonal responses to spinal cord injury. *Nat Med*. **11**:1355–1360.

Bourane S, Grossmann KS, Britz O, Dalet A, Del Barrio MG, Stam FJ, Garcia-Campmany L, Koch S, Goulding M. 2015. Identification of a spinal circuit for light touch and fine motor control. *Cell*. **160**:503–515.

Braz JM, Rico B, Basbaum AI. 2002. Transneuronal tracing of diverse CNS circuits by Cre-mediated induction of wheat germ agglutinin in transgenic mice. *Proc Natl Acad Sci USA*. **99**:15148–15153.

Callaway EM, Luo L. 2015. Monosynaptic circuit tracing with glycoprotein-deleted rabies viruses. *J Neurosci Res*. **35**:8979–8985.

Casale EJ, Light AR, Rustioni A. 1988. Direct projection of the corticospinal tract to the superficial laminae of the spinal cord in the rat. *J Comp Neurol*. **278**:275–286.

Casas-Torremocha D, Clasca F, Nunez A. 2017. Posterior thalamic nucleus modulation of tactile stimuli processing in rat motor and primary somatosensory cortices. *Front Neural Circuits*. **11**:69.

Cheng L, Duan B, Huang T, Zhang Y, Chen Y, Britz O, Garcia-Campmany L, Ren X, Vong L, Lowell BB, et al. 2017. Identification of spinal circuits involved in touch-evoked dynamic mechanical pain. *Nat Neurosci*. **20**:804–814.

Chung K, Wallace J, Kim SY, Kalyanasundaram S, Andalman AS, Davidson TJ, Mirzabekov JJ, Zalocusky KA, Mattis J, Denisin AK, et al. 2013. Structural and molecular interrogation of intact biological systems. *Nature*. **497**:332–337.

Ciabatti E, Gonzalez-Rueda A, Mariotti L, Morgese F, Tripodi M. 2017. Life-long genetic and functional access to neural circuits using self-inactivating rabies virus. *Cell*. **170**:382–392 e314.

Cichon J, Blanck TJJ, Gan WB, Yang G. 2017. Activation of cortical somatostatin interneurons prevents the development of neuropathic pain. *Nat Neurosci*. **20**:1122–1132.

Constantinople CM, Bruno RM. 2013. Deep cortical layers are activated directly by thalamus. *Science*. **340**:1591–1594.

Coudore-Civiale MA, Courteix C, Fialip J, Boucher M, Eschalier A. 2000. Spinal effect of the cholecystokinin-B receptor antagonist CI-988 on hyperalgesia, allodynia and morphine-induced analgesia in diabetic and mononeuropathic rats. *Pain*. **88**:15–22.

Del Barrio MG, Bourane S, Grossmann K, Schule R, Britsch S, O'Leary DD, Goulding M. 2013. A transcription factor code defines nine sensory interneuron subtypes in the mechanosensory area of the spinal cord. *PLoS One*. **8**: e77928.

Foster E, Wildner H, Tudeau L, Haueter S, Ralvenius WT, Jegen M, Johannssen H, Hosli L, Haenraets K, Ghanem A, et al. 2015. Targeted ablation, silencing, and activation establish glycinergic dorsal horn neurons as key components of a spinal gate for pain and itch. *Neuron*. **85**:1289–1304.

Fry EJ, Chagnon MJ, Lopez-Vales R, Tremblay ML, David S. 2010. Corticospinal tract regeneration after spinal cord injury in receptor protein tyrosine phosphatase sigma deficient mice. *Glia*. **58**:423–433.

Gerfen CR, Paletzki R, Heintz N. 2013. GENSAT BAC cre-recombinase driver lines to study the functional organization of cerebral cortical and basal ganglia circuits. *Neuron*. **80**:1368–1383.

Gilbert CD, Wiesel TN. 1979. Morphology and intracortical projections of functionally characterised neurones in the cat visual cortex. *Nature*. **280**:120–125.

Gonchar Y, Wang Q, Burkhalter A. 2007. Multiple distinct subtypes of GABAergic neurons in mouse visual cortex identified by triple immunostaining. *Front Neuroanat*. **1**:3.

Groh A, Bokor H, Mease RA, Plattner VM, Hangya B, Stroh A, Deschenes M, Acsady L. 2014. Convergence of cortical and sensory driver inputs on single thalamocortical cells. *Cereb Cortex*. **24**:3167–3179.

Gorski JA, Talley T, Qiu M, Puelles L, Rubenstein JL, Jones KR. 2002. Cortical excitatory neurons and glia, but not GABAergic neurons, are produced in the Emx1-expressing lineage. *J Neurosci*. **22**(15):6309–6314.

Haenraets K, Foster E, Johannssen H, Kandra V, Frezel N, Steffen T, Jaramillo V, Paterna JC, Zeilhofer HU, Wildner H. 2017. Spinal nociceptive circuit analysis with recombinant adeno-associated viruses: the impact of serotypes and promoters. *J Neurochem*. **142**:721–733.

Haring M, Zeisel A, Hochgerner H, Rinwa P, Jakobsson JET, Lonnerberg P, La Manno G, Sharma N, Borgius L, Kiehn O, et al. 2018. Neuronal atlas of the dorsal horn defines its architecture and links sensory input to transcriptional cell types. *Nat Neurosci*. **21**:869–880.

Harris KD, Shepherd GM. 2015. The neocortical circuit: themes and variations. *Nat Neurosci*. **18**:170–181.

Hu J, Huang T, Li T, Guo Z, Cheng L. 2012. C-Maf is required for the development of dorsal horn laminae III/IV neurons and mechanoreceptive DRG axon projections. *J Neurosci Res*. **32**:5362–5373.

Hutson TH, Verhaagen J, Yanez-Munoz RJ, Moon LD. 2012. Corticospinal tract transduction: a comparison of seven adeno-associated viral vector serotypes and a non-integrating lentiviral vector. *Gene Ther*. **19**:49–60.

Jin D, Liu YY, Sun F, Wang XH, Liu XF, He ZG. 2015. Restoration of skilled locomotion by sprouting corticospinal axons induced by co-deletion of PTEN and SOCS3. *Nat Commun*. **6**:1–12.

Jursky F, Nelson N. 1995. Localization of glycine neurotransmitter transporter (GLYT2) reveals correlation with the distribution of glycine receptor. *J Neurochem*. **64**:1026–1033.

Kamiyama T, Kameda H, Murabe N, Fukuda S, Yoshioka N, Mizukami H, Ozawa K, Sakurai M. 2015. Corticospinal tract development and spinal cord innervation differ between cervical and lumbar targets. *J Neurosci Res*. **35**:1181–1191.

Kathe C, Hutson TH, Chen Q, Shine HD, McMahon SB, Moon LD. 2014. Unilateral pyramidotomy of the corticospinal tract in rats for assessment of neuroplasticity-inducing therapies. *J Vis Exp*:1–11.

Kim EJ, Juavinett AL, Kyubwa EM, Jacobs MW, Callaway EM. 2015. Three types of cortical layer 5 neurons that differ in brain-wide connectivity and function. *Neuron*. **88**:1253–1267.

Kim J, Kim JH, Kim Y, Cho HY, Hong SK, Yoon YW. 2009. Role of spinal cholecystokinin in neuropathic pain after spinal cord hemisection in rats. *Neurosci Lett*. **462**:303–307.

Klingler E, De la Rossa A, Fievre S, Devaraju K, Abe P, Jabaudon D. 2019. A translaminar genetic logic for the circuit identity of intracortically projecting neurons. *Curr Biol*. **29**:332–339 e335.

Kovelowski CJ, Ossipov MH, Sun H, Lai J, Malan TP, Porreca F. 2000. Supraspinal cholecystokinin may drive tonic descending facilitation mechanisms to maintain neuropathic pain in the rat. *Pain*. **87**:265–273.

Lein ES, Hawrylycz MJ, Ao N, Ayres M, Bensinger A, Bernard A, Boe AF, Boguski MS, Brockway KS, Byrnes EJ, et al. 2007. Genome-wide atlas of gene expression in the adult mouse brain. *Nature*. **445**:168–176.

Lemon RN, Griffiths J. 2005. Comparing the function of the corticospinal system in different species: organizational differences for motor specialization? *Muscle Nerve*. **32**:261–279.

Liu Y, Latremoliere A, Li X, Zhang Z, Chen M, Wang X, Fang C, Zhu J, Alexandre C, Gao Z, et al. 2018. Touch and tactile neuropathic pain sensitivity are set by corticospinal projections. *Nature*. **561**:547–550.

Malmberg AB, Chen C, Tonegawa S, Basbaum AI. 1997. Preserved acute pain and reduced neuropathic pain in mice lacking PKCgamma. *Science*. **278**:279–283.

Martin WJ, Malmberg AB, Basbaum AI. 2001. PKCgamma contributes to a subset of the NMDA-dependent spinal circuits that underlie injury-induced persistent pain. *J Neurosci*. **21**:5321–5327.

McMahon S, Koltzenburg M, Tracey I, Turk D. 2013. *Ascending projection systems, Wall & Melzack's textbook of pain*. 6th ed. pp. 187–192.

Molyneaux BJ, Arlotta P, Menezes JRL, Macklis JD. 2007. Neuronal subtype specification in the cerebral cortex. *Nat Rev Neurosci*. **8**:427–437.

Muller T, Brohmann H, Pierani A, Heppenstall PA, Lewin GR, Jessell TM, Birchmeier C. 2002. The homeodomain factor lbx1 distinguishes two major programs of neuronal differentiation in the dorsal spinal cord. *Neuron*. **34**:551–562.

Peirs C, Williams SP, Zhao X, Walsh CE, Gedeon JY, Cagle NE, Goldring AC, Hioki H, Liu Z, Marell PS, et al. 2015. Dorsal horn circuits for persistent mechanical pain. *Neuron*. **87**:797–812.

Petitjean H, Pawlowski SA, Fraine SL, Sharif B, Hamad D, Fatima T, Berg J, Brown CM, Jan LY, Ribeiro-da-Silva A, et al. 2015. Dorsal horn parvalbumin neurons are gate-keepers of touch-evoked pain after nerve injury. *Cell Rep*. **13**:1246–1257.

Polgar E, Fowler JH, McGill MM, Todd AJ. 1999. The types of neuron which contain protein kinase C gamma in rat spinal cord. *Brain Res*. **833**:71–80.

Porrero C, Rubio-Garrido P, Avendano C, Clasca F. 2010. Mapping of fluorescent protein-expressing neurons and axon pathways in adult and developing Thy1-eYFP-H transgenic mice. *Brain Res*. **1345**:59–72.

Poyatos I, Ponce J, Aragon C, Gimenez C, Zafra F. 1997. The glycine transporter GLYT2 is a reliable marker for glycine-immunoreactive neurons. *Mol Brain Res*. **49**:63–70.

Quiquempoix M, Fayad SL, Boutourlinsky K, Leresche N, Lambert RC, Bessaih T. 2018. Layer 2/3 pyramidal neurons control the gain of cortical output. *Cell Rep*. **24**:2799–2807 e2794.

Roca-Lapirot O, Fossat P, Ma S, Egron K, Trigilio G, Lopez-Gonzalez MJ, Covita J, Bouali-Benazzouz R, Favereaux A, Gundlach AL, et al. 2019. Acquisition of analgesic properties by the cholecystokinin (CCK)/CCK2 receptor system within the amygdala in a persistent inflammatory pain condition. *Pain*. **160**:345–357.

Seidler B, Schmidt A, Mayr U, Nakhai H, Schmid RM, Schneider G, Saur D. 2008. A Cre-loxP-based mouse model for conditional somatic gene expression and knockdown in vivo by using avian retroviral vectors. *Proc Natl Acad Sci USA*. **105**:10137–10142.

Spike RC, Watt C, Zafra F, Todd AJ. 1997. An ultrastructural study of the glycine transporter GLYT2 and its association with glycine in the superficial laminae of the rat spinal dorsal horn. *Neuroscience*. **77**:543–551.

Steward O, Zheng B, Ho C, Anderson K, Tessier-Lavigne M. 2004. The dorsolateral corticospinal tract in mice: an alternative route for corticospinal input to caudal segments following dorsal column lesions. *J Comp Neurol*. **472**:463–477.

Steward O, Zheng B, Tessier-Lavigne M, Hofstadter M, Sharp K, Yee KM. 2008. Regenerative growth of corticospinal tract axons via the ventral column after spinal cord injury in mice. *J Neurosci*. **28**:6836–6847.

Tanaka YH, Tanaka YR, Fujiyama F, Furuta T, Yanagawa Y, Kaneko T. 2011. Local connections of layer 5 GABAergic interneurons to corticospinal neurons. *Front Neural Circuits*. **5**:12.

Taniguchi H, He M, Wu P, Kim S, Paik R, Sugino K, Kvitsiani D, Fu Y, Lu J, Lin Y, et al. 2011. A resource of Cre driver lines for genetic targeting of GABAergic neurons in cerebral cortex. *Neuron*. **71**:995–1013.

Tervo DG, Hwang BY, Viswanathan S, Gaj T, Lavzin M, Ritola KD, Lindo S, Michael S, Kuleshova E, Ojala D, et al. 2016. A designer AAV variant permits efficient retrograde access to projection neurons. *Neuron*. **92**:372–382.

Tlamsa AP, Brumberg JC. 2010. Organization and morphology of thalamocortical neurons of mouse ventral lateral thalamus. *Somatosens Mot Res*. **27**:34–43.

Ueno M, Nakamura Y, Li J, Gu Z, Niehaus J, Maezawa M, Crone SA, Goulding M, Baccei ML, Yoshida Y. 2018. Corticospinal circuits from the sensory and motor cortices differentially regulate skilled movements through distinct spinal interneurons. *Cell Rep*. **23**:1286–1300 e1287.

Voigt FF, Kirschenbaum D, Platonova E, Pages S, Campbell RAA, Kastli R, Schaettin M, Egolf L, van der Bourg A, Bethge P, et al. 2019. The mesoSPIM initiative: open-source light-sheet microscopes for imaging cleared tissue. *Nat Methods*. **16**:1105–1108.

Wang X, Liu Y, Li X, Zhang Z, Yang H, Zhang Y, Williams PR, Alwahab NSA, Kapur K, Yu B, et al. 2017. Deconstruction of corticospinal circuits for goal-directed motor skills. *Cell*. **171**:440–455 e414.

Wang Z, Maunze B, Wang Y, Tsoulfas P, Blackmore MG. 2018. Global connectivity and function of descending spinal input revealed by 3d microscopy and retrograde transduction. *J Neurosci Res*. **38**:10566–10581.

Watakabe A, Ichinohe N, Ohsawa S, Hashikawa T, Komatsu Y, Rockland KS, Yamamori T. 2007. Comparative analysis of layer-specific genes in mammalian neocortex. *Cereb Cortex*. **17**:1918–1933.

Wiesenfeld-Hallin Z, de Arauja Lucas G, Alster P, Xu XJ, Hokfelt T. 1999. Cholecystokinin/opioid interactions. *Brain Res*. **848**:78–89.

Wiesenfeld-Hallin Z, Xu XJ, Hokfelt T. 2002. The role of spinal cholecystokinin in chronic pain states. *Pharmacol Toxicol*. **91**:398–403.

Willenberg R, Steward O. 2015. Nonspecific labeling limits the utility of Cre-Lox bred CST-YFP mice for studies of corticospinal tract regeneration. *J Comp Neurol*. **523**:2665–2682.

Xu NL. 2020. Deciphering pyramidal neuron diversity: delineating perceptual functions of projection-defined neuronal types. *Neuron*. **105**:209–211.

Xu X, Roby KD, Callaway EM. 2010. Immunochemical characterization of inhibitory mouse cortical neurons: three chemically distinct classes of inhibitory cells. *J Comp Neurol*. **518**:389–404.

Zeilhofer HU, Studler B, Arabadzisz D, Schweizer C, Ahmadi S, Layh B, Bosl MR, Fritschy JM. 2005. Glycinergic neurons expressing enhanced green fluorescent protein in bacterial artificial chromosome transgenic mice. *J Comp Neurol*. **482**:123–141.

Zeisel A, Munoz-Manchado AB, Codeluppi S, Lonnerberg P, La Manno G, Jureus A, Marques S, Munguba H, He L, Betsholtz C, et al. 2015. Brain structure. Cell types in the mouse cortex and hippocampus revealed by single-cell RNA-seq. *Science*. **347**:1138–1142.